

Last Glacial Maximum ocean thermohaline circulation: PMIP2 model intercomparisons and data constraints

B. L. Otto-Bliesner,¹ C. D. Hewitt,² T. M. Marchitto,³ E. Brady,¹
A. Abe-Ouchi,^{4,5} M. Crucifix,² S. Murakami,^{5,6} and S. L. Weber⁷

Received 29 January 2007; revised 11 April 2007; accepted 4 May 2007; published 20 June 2007.

[1] The ocean thermohaline circulation is important for transports of heat and the carbon cycle. We present results from PMIP2 coupled atmosphere-ocean simulations with four climate models that are also being used for future assessments. These models give very different glacial thermohaline circulations even with comparable circulations for present. An integrated approach using results from these simulations for Last Glacial Maximum (LGM) with proxies of the state of the glacial surface and deep Atlantic supports the interpretation from nutrient tracers that the boundary between North Atlantic Deep Water and Antarctic Bottom Water was much shallower during this period. There is less constraint from this integrated reconstruction regarding the strength of the LGM North Atlantic overturning circulation, although together they suggest that it was neither appreciably stronger nor weaker than modern. Two model simulations identify a role for sea ice in both hemispheres in driving the ocean response to glacial forcing. **Citation:** Otto-Bliesner, B. L., C. D. Hewitt, T. M. Marchitto, E. Brady, A. Abe-Ouchi, M. Crucifix, S. Murakami, and S. L. Weber (2007), Last Glacial Maximum ocean thermohaline circulation: PMIP2 model intercomparisons and data constraints, *Geophys. Res. Lett.*, *34*, L12706, doi:10.1029/2007GL029475.

1. Introduction

[2] Reconstructing the strength and structure of the North Atlantic Ocean overturning circulation at the LGM is not a simple task – it is difficult enough to do for the present climate. Various paleonutrient tracers, including benthic foraminiferal $\delta^{13}\text{C}$ [Curry and Oppo, 2005; Duplessy *et al.*, 1988], Cd/Ca [Boyle, 1992; Marchitto and Broecker, 2006], Ba/Ca [Lea and Boyle, 1990], and Zn/Ca [Marchitto *et al.*, 2002], indicate that the boundary between North Atlantic Deep Water (NADW) and Antarctic Bottom Water (AABW) was substantially shallower during the LGM than today. The glacial form of NADW, named Glacial North Atlantic Inter-

mediate Water (GNAIW), occupied the Atlantic Ocean at water depths above ~ 2000 – 2500 m. This geometry was long thought to be due to a reduction in North Atlantic overturning rates compared to present day, allowing AABW to penetrate farther into the North Atlantic. In reality, however, passive nutrient tracers do not provide direct information about deep water rates [LeGrande and Wunsch, 1995].

[3] In comparison to paleonutrient tracers, sedimentary $^{231}\text{Pa}/^{230}\text{Th}$ ratios more directly reflect rates of deep water advection. $^{231}\text{Pa}/^{230}\text{Th}$ maps for the LGM imply that GNAIW was exported to the Southern Ocean at a rate similar to or slightly higher than today [Yu *et al.*, 1996]. McManus *et al.* [2004] used $^{231}\text{Pa}/^{230}\text{Th}$ from a core at Bermuda Rise to infer that the Atlantic meridional overturning circulation (MOC) was reduced by no more than ~ 30 – 40% (and probably less) during the LGM. Sediment grain size measurements also favor a rapidly flowing GNAIW during the LGM [McCave *et al.*, 1995]. These lines of evidence are seemingly at odds with a $\delta^{18}\text{O}$ -based paleogeostrophic reconstruction of the Gulf Stream through the Florida Straits, which suggests a glacial flow of only ~ 15 – 18 Sv compared to the modern 30 – 32 Sv [Lynch-Stieglitz *et al.*, 1999]. Since this flow today includes both a wind-driven gyre component of ~ 17 Sv and an MOC component of ~ 13 Sv, the LGM reconstruction implies that the MOC component was either greatly reduced or did not draw surface waters through the Straits. However, problems arise in inferring absolute LGM transports from horizontal density gradient estimates because the need to assume a level-of-no-motion [Wunsch, 2003].

[4] Further evidence of the importance of Southern Ocean deep water in the LGM North Atlantic has been derived from Ocean Drilling Program (ODP) sites from 55°N to 50°S in the Atlantic [Adkins *et al.*, 2002]. These cores yield estimates of potential temperature and salinity of the deep-ocean at LGM using pore fluid measurements of chloride concentration and $\delta^{18}\text{O}$ combined with benthic foraminiferal $\delta^{18}\text{O}$. The Atlantic sites indicate the LGM Atlantic deep waters were much colder and saltier than modern day. Deep ocean potential temperatures inferred from these cores are relatively homogeneous at LGM over the north-south extent of the Atlantic as compared to modern data. The data also suggest a significant north-south deep ocean salinity gradient at LGM in the Atlantic, with the deep Southern Ocean much saltier than the North Atlantic.

2. Models

[5] Coupled modeling studies of the LGM previously have shown widely varying changes to the LGM Atlantic meridional overturning circulation, but the interpretation of these differences has been difficult due to various forcings and

¹Climate and Global Dynamics Division, Earth and Sun Systems Laboratory, National Center for Atmospheric Research, Boulder, Colorado, USA.

²Hadley Centre for Climate Prediction and Research, Met Office, Exeter, UK.

³Department of Geological Sciences and Institute of Arctic and Alpine Research, University of Colorado, Boulder, Colorado, USA.

⁴Center for Climate System Research, University of Tokyo, Kashiwa, Japan.

⁵Frontier Research Center for Global Change, Japan Agency for Marine-Earth Science and Technology, Yokohama, Japan.

⁶Meteorological Research Institute, Tsukuba, Japan.

⁷Royal Netherlands Meteorological Institute, De Bilt, Netherlands.

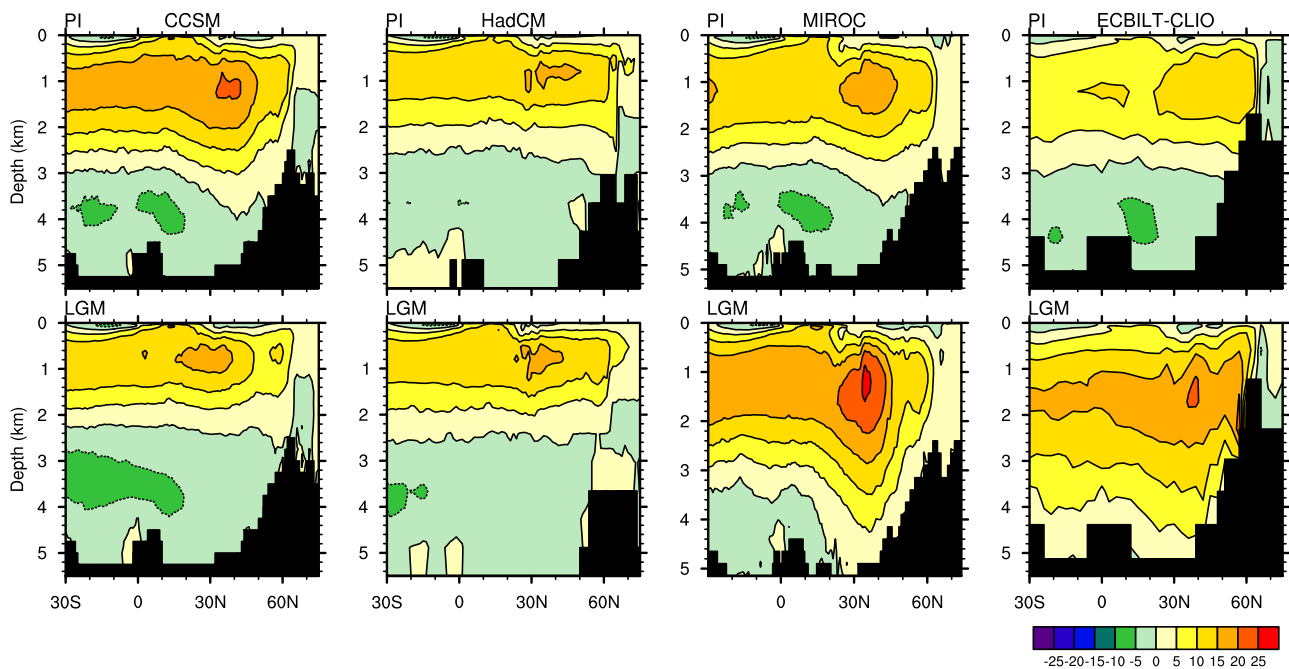


Figure 1. Atlantic Ocean meridional overturning circulations (Sv) simulated by the PMIP2 coupled atmosphere-ocean models for (top) modern and (bottom) Last Glacial Maximum.

boundary conditions used [Hewitt *et al.*, 2003; Kim, 2004; Kitoh *et al.*, 2001; Peltier and Solheim, 2004; Shin *et al.*, 2003b; Weber *et al.*, 2007]. The second phase of the Paleoclimate Modeling Intercomparison Project (PMIP2) adopts standard forcings and boundary conditions to allow model-model and model-data comparisons for the LGM [Braconnot *et al.*, 2006].

[6] For the PMIP2 LGM simulations, all of the models used the most recent reconstruction of LGM continental ice sheets, ICE-5G [Peltier, 2004], the same change from pre-industrial levels of atmospheric concentrations of carbon dioxide (CO_2), methane (CH_4), and nitrous oxide (N_2O), the specification of additional land due to a lowering of sea level, and the change to insolation resulting from a slightly different Earth's orbit. The presence of the extensive glacial ice sheets accounts for over half of the total radiative forcing of the troposphere [Hewitt and Mitchell, 1997], and the lowering of greenhouse gas concentrations (primarily the CO_2) accounts for most of the remaining radiative forcing [Otto-Bliesner *et al.*, 2006], with small contributions from the additional land and insolation changes.

[7] In this paper, we include results from four coupled climate models which have contributed PMIP2 simulations for LGM – CCSM (the National Center for Atmospheric Research CCSM3 model), HadCM (the UK Met Office HadCM3M2 model), MIROC (the CCSR/NIES/FRCGC MIROC3.2.2 (medres) model), and ECBilt-CLIO (the KNMI ECBilt/Louvain-la-Neuve CLIO intermediate complexity model) – models also used for the IPCC AR4 simulations of future climate change.

3. Results

3.1. North Atlantic Meridional Overturning Circulation

[8] These models simulate a similar modern Atlantic meridional circulation with maximum overturning strength

(below 500 m) in the North Atlantic of 13.8–20.8 Sv, within the range of observational estimates of 18 ± 3 –5 Sv [Talley *et al.*, 2003] (Figure 1). The CCSM and MIROC models show comparable depth penetration of this overturning, to 3800 m and 3500 m, respectively, at 45°N, while the HadCM3 and ECBilt simulated depth is shallower – all somewhat too shallow compared to observed estimates of ~4200 m. AABW fills the deep Atlantic below the NADW with the Atlantic portion of AABW flow of 3–4 Sv at 30°S in all models.

[9] At LGM, the four PMIP2 simulations indicate reduced (enhanced) areas of deep convection in the Nordic Seas (south of Greenland). Proxies also suggest that most GNAIW was likely formed south of Iceland [Duplessy *et al.*, 1988; Pflaumann *et al.*, 2003]. The responses of the strength of the Atlantic meridional overturning circulation differ dramatically among the models. CCSM has a modest weakening (~20%) of North Atlantic overturning strength [Otto-Bliesner *et al.*, 2006] and HadCM has only a small change in strength, while ECBilt and MIROC have increases (~20–40%) in strength. Changes in the depth of the North Atlantic overturning circulation at 45°N also show model differences. CCSM with the greatest depth at modern simulates the largest shoaling of this cell at LGM. MIROC deepens the depth of this cell at LGM to the entire depth of the model. The North Atlantic overturning cell encompasses the entire Atlantic north of 30°S in ECBilt. The HadCM model with weaker penetration of NADW at modern shows modest decreases in depth at LGM. LGM Atlantic AABW at 30°S increases in CCSM and HadCM, decreases in MIROC, and disappears in ECBilt.

3.2. Deep Ocean Temperatures and Salinities

[10] The PMIP2 models also predict the three-dimensional temperature and salinity structure of the oceans. Model-ODP comparisons show that the PMIP2 models reproduce relatively well the modern deep ocean temperature-salinity

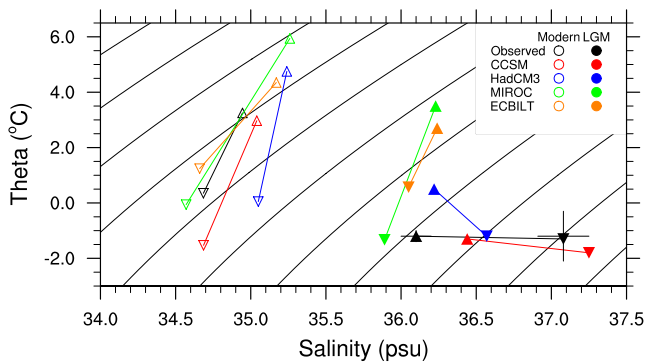


Figure 2. Temperature and salinity for modern (open symbols) and LGM (filled symbols) as estimated from data (with error bars) at ODP sites [Adkins *et al.*, 2002] and predicted by the PMIP2 models. Site 981 (triangles) is located in the North Atlantic (Feni Drift, 55°N, 15°W, 2184 m). Site 1093 (upside down triangles) is located in the South Atlantic (Shona Rise, 50°S, 6°E, 3626 m). Only CCSM included a 1 psu adjustment of ocean salinity at initialization to account for fresh water frozen into LGM ice sheets; HadCM, MIROC, and ECBilt LGM predicted salinities have been adjusted to allow comparison.

(T-S) structure in the Atlantic basin (Figure 2). The models simulate warmer and saltier deep waters at Feni Drift in the North Atlantic than at Shona Rise in the Atlantic sector of the Southern Ocean. Thus, for all the models the NADW is warmer and saltier than the AABW and deep ocean density gradients are mainly due to the temperature difference at modern day.

[11] Greater differences between models occur for the LGM simulations. CCSM and somewhat HadCM simulate the different observed north-south T-S structure for the LGM deep ocean. LGM deep waters simulated by these two models are very cold ($<0^{\circ}\text{C}$) and have relatively homogeneous temperature-structure from north to south in the Atlantic basin (see auxiliary material).¹ CCSM simulates the observed large north-south salinity differences at LGM (auxiliary material). The MIROC and ECBilt models also simulate colder LGM deep waters and simulate somewhat greater salinity increases in the Southern Ocean than the North Atlantic as compared to modern, but retain the temperature-salinity structure as the modern simulation.

3.3. Water Mass Formation

[12] Several mechanisms have been proposed to explain the Atlantic THC response at LGM, including changes in net evaporation over the Atlantic basin [Schmittner *et al.*, 2002] and the density contrast between AABW and NADW [Shin *et al.*, 2003a]. Weber *et al.* [2007] showed that only in HadCM does a net reduction in evaporation over the Atlantic basin play a dominant role. Two of the PMIP2 models, CCSM and MIROC, were shown to have significant, but of opposite sign, response to the density contrast between AABW and NADW. These two models have

similar resolutions of the atmosphere and ocean components, similar modern Atlantic meridional overturning circulations, while they are at the far ends of the simulated glacial Atlantic meridional overturning circulations. To understand these differing responses, we calculate the water mass formation rates (WMF) to represent the effects of the thermal and haline buoyancy fluxes on the surface density fields (Table 1). Ocean surface buoyancy fluxes in the subpolar regions, from thermal forcing by heat fluxes at the surface and haline forcing by freshwater fluxes, drive water mass formation rates of NADW, GNAIW, and AABW.

[13] For modern, the North Atlantic WMF contributions to the NADW, associated with winter heat losses and cooling of the North Atlantic surface ocean, dominate in both CCSM and MIROC, with the haline contributions smaller and partly offsetting the thermal contribution. For LGM, the haline contributions to North Atlantic WMF remain small in both models. The thermal contributions, on the other hand, show opposite tendencies at LGM between the two models. CCSM has $\sim 30\%$ reduction in the thermal and total forcing of North Atlantic WMF. MIROC has a $\sim 60\%$ increase in the thermal forcing and total rate of North Atlantic WMF.

[14] The Southern Ocean WMF contributes to the AABW found in the deepest parts of all three ocean basins, particularly near the south. For modern, the haline contribution due to brine rejection with production of sea ice in the Weddell and Ross Seas dominates over the thermal contribution in CCSM. The opposite is true in the MIROC model with the thermal contribution to modern Southern Ocean WMF larger than the haline contribution. Large differences of Southern Ocean WMF between the two models occur at LGM. Both models exhibit decreases in the thermal contribution and increases in the haline contribution to Southern Ocean WMF at LGM, but CCSM has a much larger haline contribution. The total rate of LGM Southern Ocean WMF is two times greater in CCSM than MIROC and as a result the AABW extends farther northward at LGM in all three basins.

3.4. Sea Ice

[15] Sea ice plays an important role for understanding the different responses of the thermohaline circulation to glacial forcing in the CCSM and MIROC models. The thermal contributions are most important for North Atlantic WMF at LGM in both models, but for CCSM this contribution is only about half that of MIROC. WMF due to heat loss occurs in the sea ice-free regions where high surface densities are coincident with large thermal buoyancy forcing. In the MIROC model, the absence of winter ice south of Greenland at LGM allows large heat exchange between the ocean and atmosphere, especially during the winter months (Figure 3). CCSM has more extensive winter sea ice in the North Atlantic, especially in the western North Atlantic south of Greenland-Iceland. Regions of WMF in CCSM at LGM occur south of Greenland and also in a northward seasonally sea ice-free region in the Greenland-Iceland-Norwegian Sea but the thermal buoyancy forcing is smaller than in MIROC in these regions.

[16] In the Southern Ocean, brine rejection due to sea ice production increases the densification of the waters around Antarctica. Seasonally, the largest brine rejection occurs

¹Auxiliary materials are available in the HTML. doi:10.1029/2007GL029475.

Table 1. High-Latitude, Deep Water Mass Formation Rates for Southern Ocean and Northern North Atlantic Ocean in Total and Split Into the Haline and Thermal Contributions as Simulated for Modern and LGM by the CCSM and MIROC Models^a

	CCSM: T42 Atmosphere $0.3-1^\circ \times 1^\circ$ Ocean		MIROC: T42 Atmosphere $0.5-1.4^\circ \times 1.4^\circ$ Ocean	
	Modern	LGM	Modern	LGM
Southern Ocean				
Haline contribution	11.1 (27.7)	39.6 (29.9)	2.3 (27.8)	11.8 (27.8)
Thermal contribution	5.1 (27.7)	0.4 (29.9)	15.8 (27.6)	7.8 (27.8)
Total	16.2 (27.7)	40.0 (29.9)	10.4 (27.5)	19.6 (27.8)
Northern North Atlantic				
Haline contribution	-5.9 (27.5)	2.3 (29.3)	-5.2 (27.4)	1.7 (28.2)
Thermal contribution	24.4 (27.5)	16.6 (29.0)	24.2 (27.5)	35.5 (27.7)
Total	18.6 (27.5)	13.9 (29.0)	19.4 (27.5)	30.7 (27.9)

^aWater mass formation rates are given in Sv ($1 \text{ Sv} = 10^6 \text{ m}^3 \text{ s}^{-1}$). Haline and thermal contributions are calculated as by *Bryan et al.* [2006]. Positive (negative) WMFs indicate a net transport into (out of) water denser than the density anomalies σ_θ indicated in parentheses. The thermal and haline contributions to WMF separate in both space and density class in climate models with active sea ice components [*Doney et al.*, 1998].

where sea ice is being formed, i.e. in open ice leads in coastal regions and just off the permanent ice. CCSM has vigorous seasonal sea ice formation and export at LGM around Antarctica. The result is a significant increase in WMF of AABW in the CCSM simulation at LGM as compared to modern. MIROC, on the other hand, has less extensive LGM sea ice and a more modest haline contribution to WMF.

4. Summary and Conclusions

[17] The LGM North Atlantic MOC changes in the PMIP2 models fall into three classes: shallower but less

confidently weaker (CCSM), no significant changes (HadCM), and deeper and stronger (MIROC and ECBilt). For CCSM and MIROC, the responses are tied to the buoyancy fluxes in the North Atlantic and Southern Ocean. Differences are related to more seasonally extensive sea ice at LGM in CCSM than MIROC. HadCM and ECBilt have more intermediate changes in LGM sea ice extent (auxiliary material), though in neither does density contrast between AABW and NADW play a controlling role in determining the strength of LGM NADW [*Weber et al.*, 2007].

[18] Proxy reconstructions of LGM sea ice and ocean stratification can provide additional constraints on interpre-

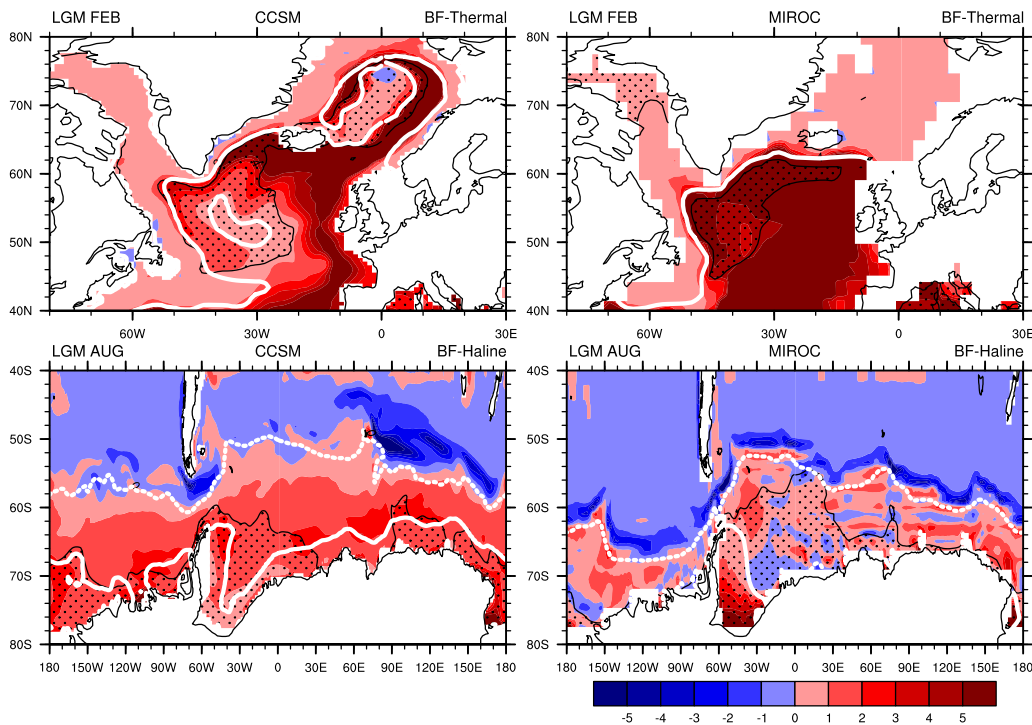


Figure 3. The buoyancy forcing ($10^{-6} \text{ kg} \cdot \text{m}^{-2} \cdot \text{s}^{-1}$) at LGM predicted by CCSM and MIROC for (top) northern winter (February) by the thermal contribution in the North Atlantic and (bottom) southern winter (August) by the haline contribution in the Southern Ocean. Regions of high density for each model where deep water mass formation occurs are dotted. The white lines indicate (top) the model LGM February sea ice edge, 50% concentration, representing northern winter extent, and (bottom) LGM February (solid) and September (dotted) sea ice edges, 90% concentration, representing permanent and winter Southern Hemisphere extents.

tation of the LGM Atlantic meridional overturning. LGM AABW forms in coastal leads and just equatorward of permanent sea ice cover due to brine rejection during sea ice production [Shin *et al.*, 2003a]. Southern Ocean summer sea ice extent simulated at LGM by CCSM closely follows the summer sea ice edge in the Atlantic sector as reconstructed by CLIMAP Project Members [1981] and EPILOG [Gersonde *et al.*, 2005]. The CCSM LGM simulation of Southern Hemisphere sea ice and deep Atlantic temperature and salinity as compared to proxy records confirms the interpretation from paleonutrient tracers and previous modeling that the glacial Atlantic Ocean was more stably stratified at high northern latitudes with a shoaling of NADW (i.e. GNAIW), and AABW penetrating much farther into the North Atlantic than present.

[19] The continental ice sheets over North America and the extensive sea ice over the Labrador Sea create a source of cold, dry air which enhances the cooling and evaporation downstream over the North Atlantic. Sea ice extent has been shown to be crucial to modulating the impact of atmospheric forcing and thus water mass formation in the subpolar North Atlantic at LGM in an eddy-permitting ocean model [Yang *et al.*, 2006]. CCSM overestimates proxy evidence of LGM winter sea ice in the region south of Greenland [CLIMAP Project Members, 1981; Sarnthein *et al.*, 2003], a region at modern of large upward heat flux from the ocean to atmosphere, and so may underestimate production of GNAIW. MIROC underestimates proxy evidence of sea ice indicating production of LGM NADW may be overestimated. The model results for the strength of GNAIW and proxy evidence from a variety of tracers suggests GNAIW was not significantly stronger than modern and perhaps not considerably weaker either.

[20] The strength of NADW and suppression of air-sea gas exchange due to glacial sea ice expansion in the Southern Ocean have been suggested as playing possible roles in regulating past atmospheric CO₂. In turn, climate model results indicate that lower glacial CO₂ can effect substantial changes to sea ice and the glacial thermohaline circulation. Thus, a reconstruction of Atlantic overturning circulation, ocean stratification, and sea ice extent is critical to understanding the biogeochemical and physical feedbacks that regulate the past carbon cycle.

[21] **Acknowledgments.** We acknowledge the international modeling groups for providing their data for analysis, the Laboratoire des Sciences du Climat et de l'Environnement for collecting and archiving the model data. The PMIP2/MOTIF Data Archive is supported by CEA, CNRS, the EU project MOTIF, and the Programme National d'Etude de la Dynamique du Climat. Funding for NCAR and this research was provided by NSF.

References

- Adkins, J. F., K. McIntyre, and D. P. Schrag (2002), The salinity, temperature, and $\delta^{18}\text{O}$ of the glacial deep ocean, *Science*, *298*, 1769–1773.
- Boyle, E. A. (1992), Cadmium and $\delta^{13}\text{C}$ paleochemical ocean distributions during the stage 2 glacial maximum, *Annu. Rev. Earth Planet. Sci.*, *20*, 245–287.
- Braconnot, P., et al. (2006), Coupled simulations of the mid-Holocene and Last Glacial Maximum: New results from PMIP2, *Clim. Past Discuss.*, *2*, 1293–1346.
- Bryan, F., et al. (2006), Response of North Atlantic thermohaline circulation and ventilation to increasing carbon dioxide in CCSM3, *J. Clim.*, *19*, 2382–2397.
- CLIMAP Project Members (1981), Seasonal reconstructions of the Earth's surface at the Last Glacial Maximum, *Map Chart Ser. MC-36*, 18 pp., Geol. Soc. of Am., Boulder, Colo.
- Curry, W. B., and D. W. Oppo (2005), Glacial water mass geometry and the distribution of $\delta^{13}\text{C}$ of ΣCO_2 in the western Atlantic Ocean, *Paleoceanography*, *20*, PA1017, doi:10.1029/2004PA001021.
- Doney, S. C., W. G. Large, and F. O. Bryan (1998), Surface ocean fluxes and water-mass transformation rates in the coupled NCAR Climate System Model, *J. Clim.*, *11*, 1420–1441.
- Duplessy, J. C., N. J. Shackleton, R. G. Fairbanks, L. Labeyrie, D. Oppo, and N. Kallel (1988), Deep water source variations during the last climatic cycle and their impact on the global deep water circulation, *Paleoceanography*, *3*, 343–360.
- Gersonde, R., X. Crosta, A. Abelmann, and L. Armand (2005), Sea-surface temperature and sea ice distribution of the Southern Ocean at the EPILOG Last Glacial Maximum—A circum-Antarctic view based on siliceous microfossil records, *Quat. Sci. Rev.*, *24*, 869–896.
- Hewitt, C. D., and J. F. B. Mitchell (1997), Radiative forcing and response of a GCM to ice age boundary conditions: Cloud feedback and climate sensitivity, *Clim. Dyn.*, *13*, 821–834.
- Hewitt, C. D., R. J. Stouffer, A. J. Broccoli, J. F. B. Mitchell, and P. J. Valdes (2003), The effect of ocean dynamics in a coupled GCM simulation of the Last Glacial Maximum, *Clim. Dyn.*, *20*, 203–218.
- Kim, S.-J. (2004), A coupled model simulation of ocean thermohaline properties of the Last Glacial Maximum, *Atmos. Ocean*, *42*, 213–220.
- Kitoh, A., S. Murakami, and H. Koide (2001), A simulation of the Last Glacial Maximum with a coupled atmosphere-ocean GCM, *Geophys. Res. Lett.*, *28*, 2221–2224.
- Lea, D. W., and E. A. Boyle (1990), Foraminiferal reconstruction of barium distributions in water masses of the glacial oceans, *Paleoceanography*, *5*, 712–742.
- LeGrande, P., and C. Wunsch (1995), Constraints from paleotracer data on the North Atlantic circulation during the Last Glacial Maximum, *Paleoceanography*, *10*, 1011–1046.
- Lynch-Stieglitz, J., W. B. Curry, and N. Slowey (1999), Weaker Gulf Stream in the Florida Straits during the Last Glacial Maximum, *Nature*, *402*, 644–648.
- Marchitto, T. M., and W. S. Broecker (2006), Deep water mass geometry in the glacial Atlantic Ocean: A review of constraints from the paleonutrient proxy Cd/Ca, *Geochem. Geophys. Geosyst.*, *7*, Q12003, doi:10.1029/2006GC001323.
- Marchitto, T. M., Jr., D. W. Oppo, and W. B. Curry (2002), Paired benthic foraminiferal Cd/Ca and Zn/Ca evidence for a greatly increased presence of Southern Ocean Water in the glacial North Atlantic, *Paleoceanography*, *17*(3), 1038, doi:10.1029/2000PA000598.
- McCave, I. N., B. Manighetti, and N. A. S. Beveridge (1995), Circulation in the glacial North Atlantic inferred from grain-size measurements, *Nature*, *374*, 149–151.
- McManus, J. F., R. Francois, J.-M. Gherardi, L. Keigwin, and S. Brown-Leger (2004), Collapse and rapid resumption of Atlantic meridional circulation linked to deglacial climate changes, *Nature*, *428*, 834–837.
- Otto-Bliesner, B. L., et al. (2006), Last Glacial Maximum and Holocene climate in CCSM3, *J. Clim.*, *19*, 2567–2583.
- Peltier, W. R. (2004), Global glacial isostasy and the surface of the ice-age Earth: The ICE-5G (VM2) model and GRACE, *Annu. Rev. Earth Planet. Sci.*, *32*, 111–149.
- Peltier, W. R., and L. P. Solheim (2004), The climate of the Earth at Last Glacial Maximum: Statistical equilibrium state and a mode of internal variability, *Quat. Sci. Rev.*, *23*, 335–357.
- Pflaumann, U., et al. (2003), Glacial North Atlantic: Sea-surface conditions reconstructed by GLAMAP 2000, *Paleoceanography*, *18*(3), 1065, doi:10.1029/2002PA000774.
- Sarnthein, M., U. Pflaumann, and M. Weinelt (2003), Past extent of sea ice in the northern North Atlantic inferred from foraminiferal paleotemperature estimates, *Paleoceanography*, *18*(2), 1047, doi:10.1029/2002PA000771.
- Schmittner, A., K. J. Meissner, M. Eby, and A. J. Weaver (2002), Forcing of the deep ocean circulation in simulations of the Last Glacial Maximum, *Paleoceanography*, *17*(2), 1015, doi:10.1029/2001PA000633.
- Shin, S.-I., Z. Liu, B. L. Otto-Bliesner, J. E. Kutzbach, and S. J. Vavrus (2003a), Southern Ocean sea-ice control of the glacial North Atlantic thermohaline circulation, *Geophys. Res. Lett.*, *30*(2), 1096, doi:10.1029/2002GL015513.
- Shin, S.-I., et al. (2003b), A simulation of the Last Glacial Maximum climate using the NCAR CSM, *Clim. Dyn.*, *20*, 127–151.
- Talley, L., J. Reid, and P. Robbins (2003), Data-based meridional overturning streamfunctions for the global ocean, *J. Clim.*, *16*, 3213–3226.
- Weber, S. L., et al. (2007), The modern and glacial overturning circulation in the Atlantic Ocean in PMIP coupled model simulations, *Clim. Past*, *3*, 51–64.
- Wunsch, C. (2003), Determining paleoceanographic circulations, with emphasis on the Last Glacial Maximum, *Quat. Sci. Rev.*, *22*, 371–385.

Yang, D., P. G. Myers, and A. B. G. Bush (2006), Sensitivity of the sub-polar North Atlantic to Last Glacial Maximum surface forcing and sea ice distribution in an eddy-permitting regional ocean model, *Paleoceanography*, 21, PA2013, doi:10.1029/2005PA001209.

Yu, E.-F., R. Francois, and P. Bacon (1996), Similar rates of modern and last-glacial ocean thermohaline circulation inferred from radiochemical data, *Nature*, 379, 689–694.

A. Abe-Ouchi, Center for Climate System Research, University of Tokyo, 5-1-5 Kashiwanoha, Chiba, Kashiwa 277-8568, Japan.

E. Brady and B. L. Otto-Bliesner, Climate and Global Dynamics Division, Earth and Sun Systems Laboratory, National Center for Atmo-

spheric Research, P.O. Box 3000, Boulder, CO 80307, USA. (ottobli@ucar.edu)

M. Crucifix and C. D. Hewitt, Hadley Centre for Climate Prediction and Research, Met Office, FitzRoy Road, Exeter EX1 3PB, UK.

T. M. Marchitto, Department of Geological Sciences and Institute of Arctic and Alpine Research, University of Colorado, Campus Box 450, Boulder, CO 80309-0450, USA.

S. Murakami, Meteorological Research Institute, Nagamine 1-1, Ibaraki, Tsukuba 305-0052, Japan.

S. L. Weber, Royal Netherlands Meteorological Institute, P.O. Box 201, NL-3730 A E De Bilt, Netherlands.